Table 4 Accuracy of elastography determined by receiver operating characteristic (ROC) analysis stratified by inflammatory activity (a) and steatosis (b) of the liver biopsy specimen (* $p < 0.05$ by χ^2 analysis)

	Fibroscan®						ARFI-R					
	Activity 0–1 ($n = 57$)			Activity 2–3 ($n = 52$)			Activity 0–1 ($n = 59$)			Activity 2–3 ($n = 54$)		
	AUC	Cut-off value	LR	AUC	Cut-off value	LR	AUC	Cut-off value	LR	AUC	Cut-off value	LR
(a) Inflammatory activity												
F0 vs. F1–4	0.802	6.3	3.60	0.511	6.2	1.13	0.865*	1.05	5.19	0.495	1.00	1.31
F0–1 vs. F2–4	0.899*	9.1	4.28	0.861*	11.6	3.95	0.889*	1.30	3.01	0.839*	1.51	2.69
F0–2 vs. F3–4	0.936*	11.7	4.69	0.867*	11.6	3.33	0.918*	1.67	5.25	0.854*	1.80	3.89
F0–3 vs. F4	0.901*	17.5	8.05	0.860*	20.3	8.06	0.874*	1.88	4.32	0.735*	2.00	3.07
	Fibroscan®						ARFI-R					
	Steatosis 0–1 ($n = 80$)			Steatosis 2–3 ($n = 29$)			Steatosis 0–1 ($n = 82$)			Steatosis 2–3 ($n = 31$)		
	AUC	Cut-off value	LR	AUC	Cut-off value	LR	AUC	Cut-off value	LR	AUC	Cut-off value	LR
(b) Steatosis												
F0 vs. F1–4	0.647	6.3	1.65	0.793	6.7	2.16	0.726	1.02	2.21	0.741	1.02	2.33
F0–1 vs. F2–4	0.867*	9.1	2.61	0.957*	12.3	8.50	0.854*	1.35	2.22	0.900*	1.30	3.80
F0–2 vs. F3–4	0.894*	11.6	4.06	0.933*	12.3	6.00	0.870*	1.65	3.96	0.920*	1.53	4.00
F0–3 vs. F4	0.872*	17.5	5.08	0.935*	18.8	9.20	0.782*	1.88	3.49	0.896*	2.19	6.25

differentiate accurately between F3 and F4 by observing specimens obtained by liver needle biopsy, and pathological findings could sometimes underestimate the actual fibrosis. The cut-off values obtained by ROC analysis for differentiating F0–3 from F4 were 14.3 kPa and 1.88 m/s, respectively. These data were similar to those described in previous reports [23, 24, 26]. Liver biopsy is not suitable for repeated evaluations because it is invasive and can cause major complications (0.3–0.5%), including death (0.03–0.1%) [5]. Moreover, liver fibrosis is a sequential and/or continuous process, and the staging of liver fibrosis should be evaluated frequently. In contrast to liver biopsy, transient elastography is non-invasive and can be repeated many times in the same patient. This feature is very useful clinically. Masuzaki et al. [27] prospectively studied the efficacy of Fibroscan® in predicting HCC development in patients with chronic hepatitis C, and demonstrated encouraging results. Thus, transient elastography provides a new procedure to assess and predict some of the clinical signs of chronic liver disease.

In the present study, we compared values of ARFI to the values with the Fibroscan® method. ARFI was superior in terms of its convenience because it is equipped with US. In this study, ARFI could be performed on all patients, while Fibroscan® failed for 4 patients because of the presence of thick subcutaneous fat tissue and/or liver atrophy. These drawbacks have been pointed out previously [28]. Moreover, the accuracy of diagnosing the stages of fibrosis by ARFI is similar to that with the Fibroscan® method and is considered to be satisfactory, although differentiation of the existence of slight fibrosis was deemed to be insufficient. Recently Lupsor et al. [11] reported preliminary results for a study comparing the ARFI and Fibroscan® methods in patients with chronic hepatitis C. They found that both ARFI and Fibroscan® data were strongly correlated with the stage of fibrosis, and Fibroscan® was better for predictions of earlier stages. However, our prospective study incorporated a percutaneous liver biopsy taken at the same time as the elastography measurements, and we did not find that the Fibroscan® method was superior in the earlier stages.

In conclusion, we evaluated the utility of transient elastography by ARFI for the diagnosis of liver fibrosis and found that the ARFI data correlated significantly with fibrosis staging. Although there are several issues that should be considered carefully in the future (such as inflammation), we conclude that transient elastography with ARFI method, as well as Fibroscan®, is a very simple, non-invasive, and useful procedure in the field of hepatology.

References

1. Manning DS, Afdhal NH. Diagnosis and quantitation of fibrosis. Gastroenterology. 2008;134:1670–81.
2. Sherlock S. Aspiration liver biopsy, technique and diagnostic application. Lancet. 1945;ii:397.

3. Regev A, Berho M, Jeffers LJ, Milikowski C, Molina EG, Pyrsopoulos NT, et al. Sampling error and intraobserver variation in liver biopsy in patients with chronic HCV infection. Am J Gastroenterol. 2002;97:2614–8.
4. Bedossa P, Dargere D, Paradis V. Sampling variability of liver fibrosis in chronic hepatitis C. Hepatology. 2003;38:1449–57.
5. Dienstag JL. The role of liver biopsy in chronic hepatitis C. Hepatology. 2002;36:S152–60.
6. Poniachik J, Bernstein DE, Reddy KR, Jeffers LJ, Coelho-Little ME, Civantos F, et al. The role of laparoscopy in the diagnosis of cirrhosis. Gastrointest Endosc. 1996;43:568–71.
7. Sandrin L, Fourquet B, Hasquenoph JM, Yon S, Fournier C, Mal F, et al. Transient elastography: a new noninvasive method for assessment of hepatic fibrosis. Ultrasound Med Biol. 2003;29:1705–13.
8. Saito H, Tada S, Nakamoto N, Kitamura K, Horikawa H, Kurita S, et al. Efficacy of non-invasive elastometry on staging of hepatic fibrosis. Hepatol Res. 2004;29:97–103.
9. Fahey BJ, Nightingale KR, Nelson RC, Palmeri ML, Trahey GE. Acoustic radiation force impulse imaging of the abdomen: demonstration of feasibility and utility. Ultrasound Med Biol. 2005;31:1185–98.
10. Palmeri ML, Wang MH, Dahl JJ, Frinkley KD, Nightingale KR. Quantifying hepatic shear modulus in vivo using acoustic radiation force. Ultrasound Med Biol. 2008;34:546–58.
11. Lupsor M, Badea R, Stefanescu H, Sparchez Z, Branda H, Serban A, et al. Performance of a new elastographic method (ARFI technology) compared to unidimensional transient elastography in the noninvasive assessment of chronic hepatitis C. Preliminary results. J Gastrointestin Liver Dis. 2009;18:303–10.
12. The French METAVIR Cooperative Study Group. Intraobserver and interobserver variations in liver biopsy interpretation in patients with chronic hepatitis C. Hepatology. 1994;20:15–20.
13. Brunt EM. Nonalcoholic steatohepatitis: definition and pathology. Semin Liver Dis. 2001;21:3–16.
14. Sagir A, Erhardt A, Schmitt M, Häussinger D. Transient elastography is unreliable for detection of cirrhosis in patients with acute liver damage. Hepatology. 2008;47:592–5.
15. Arena U, Vizzutti F, Corti G, Ambu S, Stasi C, Bresci S, et al. Acute viral hepatitis increases liver stiffness values measured by transient elastography. Hepatology. 2008;47:380–4.
16. Nightingale RK, Soo MS, Nightingale R, Trahey G. Acoustic radiation force impulse imaging: in vivo demonstration of clinical feasibility. Ultrasound Med Biol. 2002;28:227–35.
17. Palmeri ML, Frinkley KD, Zhai L, Gottfried M, Bentley RC, Ludwig K. Acoustic radiation force impulse (ARFI) imaging of the gastrointestinal tract. Ultrason Imaging. 2005;27:75–88.
18. Sarvazyan AP, Rudenko OV, Swanson SD, Fowlkes JB, Emelianov SY. Shear wave elasticity imaging: a new ultrasonic technology of medical diagnostics. Ultrasound Med Biol. 1998;24:1419–35.
19. Wai CT, Greenson JK, Fontana RJ, Kalbfleisch JD, Marrero JA, Conjeevaram HS, et al. A simple noninvasive index can predict both significant fibrosis and cirrhosis in patients with chronic hepatitis C. Hepatology. 2003;38:518–26.
20. Imbert-Bismut F, Ratziu V, Pieroni L, Charlotte F, Benhamou Y, Poynard T, et al. Biochemical markers of liver fibrosis in patients with hepatitis C virus infection: a prospective study. Lancet. 2001;357:1069–75.
21. Talwalkar JA, Kurtz DM, Schoenleber SJ, West CP, Montori VM. Ultrasound-based transient elastography for the detection of hepatic fibrosis: systematic review and meta-analysis. Clin Gastroenterol Hepatol. 2007;5:1214–20.
22. Friedrich-Rust M, Ong MF, Martens S, Sarrazin C, Bojunga J, Zeuzem S, et al. Performance of transient elastography for the staging of liver fibrosis: a meta-analysis. Gastroenterology. 2008;134:960–74.
23. Foucher J, Chanteloup E, Vergniol J, Caste′ra L, Le Bail B, Adhoute X et al. Diagnosis of cirrhosis by transient elastography (FibroScan): a prospective study. Gut. 2006;55:403–8.
24. Kim KM, Choi W-B, Park SH, Yu E, Lee SG, Lim Y-S, et al. Diagnosis of hepatic steatosis and fibrosis by transient elastography in asymptomatic healthy individuals: a prospective study of living related potential liver donors. J Gastroenterol. 2007;42:382–8.
25. Iijima H. The usefulness of non-invasive diagnosis of liver fibrosis using acoustic radiation force impulse. Kanzo. 2010;51:54–5.
26. Obara N, Ueno Y, Fukushima K, Nakagome Y, Kakazu E, Kimura O, et al. Transient elastography for measurement of liver stiffness measurement can detect early significant hepatic fibrosis in Japanese patients with viral and nonviral liver diseases. J Gastroenterol. 2008;43:720–8.
27. Masuzaki R, Tateishi R, Yoshida H, Goto E, Sato T, Ohki T, et al. Prospective risk assessment for hepatocellular carcinoma development in patients with chronic hepatitis C by transient elastography. Hepatology. 2009;49:1954–61.
28. Kettaneh A, Marcellin P, Douvin C, Poupon R, Ziol M, Beaugrand M, et al. Features associated with success rate and performance of FibroScan measurements for the diagnosis of cirrhosis in HCV patients: a prospective study of 935 patients. J Hepatol. 2007;46:628–34.

Digestive Diseases

Dig Dis 2011;29:284–288
DOI: 10.1159/000327560

Molecular Pathogenesis of Hepatocellular Carcinoma: Altering Transforming Growth Factor-β Signaling in Hepatocarcinogenesis

Ken Yamazaki Yohei Masugi Michiie Sakamoto

Department of Pathology, School of Medicine, Keio University, Tokyo, Japan

Key Words

Hepatocellular carcinoma · Multistep carcinogenesis · TGF-β signaling · Microenvironment · Tumor-stromal interaction · Hepatocyte growth factor

Abstract

Hepatocellular carcinoma (HCC) occurs subsequent to liver injury, where regenerative hepatocytes develop into a dysplastic nodule and then early HCC, supporting the multistep hepatocarcinogenesis theory. Molecular alterations such as the *p53* mutation, *p16* gene silencing, and AKT signaling activation are found in the late stage of HCC progression. The overexpression of some marker molecules is observed at the early stage. Transforming growth factor-β (TGF-β), a potent inhibitor of cell proliferation, is frequently overexpressed in HCC, although the role of TGF-β signaling during HCC development remains controversial. We previously reported that HCC cells show TGF-β receptor-dependent growth inhibition in response to TGF-β. Also, reduced TGF-β receptor II in HCC correlates with intrahepatic metastasis and shorter time-to-recurrence, suggesting a role of TGF-β signaling in tumor suppression. In contrast, TGF-β overexpression in HCC is known to correlate with malignant potential, suggesting a role in tumor promotion. Enhanced formation of stroma is a feature of advanced HCC, and TGF-β also promotes the proliferation of stromal fibroblasts. The microenvironment produced via tumor-stromal interactions may be the key to the modulation of the dual roles of TGF-β signaling in HCC progression.

Multistep Hepatocarcinogenesis

Hepatocellular carcinoma (HCC) is the fourth leading cause of cancer death worldwide [1]. The incidence of HCC differs between geographical regions, and is closely related to the prevalence of chronic infection. Most HCCs develop following chronic liver disease caused by a hepatitis B virus (HBV) and/or hepatitis C virus (HCV) [2] infection. Clinical, radiological, and pathological findings indicate a multistep process in the development of HCC. Dysplastic nodules (DN) are usually found in the liver with chronic inflammation, and will eventually develop into early HCC. The transitional progress from an early to more advanced stage is histologically described as a nodule-in-nodule lesion, where moderately or poorly differentiated tumor grows within a well-differentiated cancer nodule. Advanced HCC often shows intrahepatic metastasis disseminated through portal vein invasion, indicating a poor prognosis. To understand the multistep progression of HCC, molecular alterations can serve as signs for the transition of each step.

Molecular Alterations in HCC

Gene mutations are a crucial molecular alteration in many cancers, and the *p53* gene is the most frequently mutated in HCC. Oda et al. [3] demonstrated mutations of the *p53* gene in poorly differentiated tumor components of a nodule-in-nodule type HCC, but no mutation in a well-

KARGER

Fax +41 61 306 12 34
E-Mail karger@karger.ch
www.karger.com

0257–2753/11/0293–0284$38.00/0

Accessible online at:
www.karger.com/ddi

Michiie Sakamoto, MD, PhD
Department of Pathology, School of Medicine, Keio University
35 Shinanomachi, Shinjuku-ku
Tokyo 160-8582 (Japan)
Tel. +81 3 5363 3762, E-Mail msakamot@sc.itc.keio.ac.jp

differentiated tumor component surrounding the former [3]. Nuclear accumulation of mutated p53 is immunohistochemically detected in HCCs, and is correlated with tumor grade and size [4]. These findings indicate that the *p53* gene mutation occurs at a later stage in HCC progression.

Epigenetic silencing contributes molecular alterations without gene mutation/deletion in cancer. The *p16* (*CDKN2A*) tumor suppressor gene encodes a cyclin-dependent kinase inhibitor that is involved in the cell cycle regulatory pathway. Suppressed *p16* expression in HCC is mainly due to hypermethylation of the gene [5]. Loss of p16 protein occurs approximately twice as often in advanced HCCs (40%) than in early HCCs [5].

Aberrant activation of signal transduction is another molecular alteration in cancer. AKT/PKB phosphorylation has been identified as a significant risk factor for an early recurrence and poor prognosis in HCC [6].

The molecular alterations described above are rare in the early stages of HCC progression, however molecular markers upregulated in the early stages have been reported. Heat-shock protein 70 and adenylate cyclase-associated protein 2 are detected in early HCC, and are highly expressed in advanced HCC [7, 8]. Since these molecules show a stepwise upregulation with HCC progression, they can serve as useful markers for HCC diagnosis.

Molecular markers detectable in the blood are useful for less invasive diagnoses. Plasma α-fetoprotein levels have been an important factor in the diagnosis and prognosis of HCC. Elevated levels of plasma TGF-β in HCC patients have been reported [9], but may not be specific for HCC due to upregulation in the inflamed liver. While TGF-β is a cell growth inhibitor, its overexpression in HCC correlates with carcinogenesis, progression, and prognosis [10–12]. Indeed, the role of TGF-β signaling in HCC is controversial. Recently, we showed that reduced TGF-β receptor type II (TGFBR2) expression in HCC correlated with intrahepatic metastasis and shorter time to recurrence [13]. Various roles of TGF-β signaling may be implicated in multistep hepatocarcinogenesis.

Canonical TGF-β Signaling

The TGF-β superfamily contains molecules with a diverse range of functions in embryogenesis and adult tissue homeostasis. TGF-β ligand binds with a heteromeric receptor complex that consists of type I and type II serine/threonine kinase receptors. Upon ligand-receptor binding, the type I receptor phosphorylates receptor-activated SMAD (R-SMAD) proteins at their C-terminal serines. SMAD is a TGF-β signaling transducer with conserved MAD-homology (MH) 1, an intermediate linker, and MH2 regions. The activated R-SMADs, together with SMAD4, translocate into the nucleus and function as a transcription factor complex. One of the target genes of TGF-β, SMAD7, encodes an inhibitory SMAD that binds to the type I TGF-β receptor and competitively blocks the interaction between the TGF-β receptor and R-SMAD [14].

The regenerative potential of the liver has been recognized since ancient times and the regenerative capacity of hepatocytes is exploited in the recovery from liver injury. TGF-β signaling plays a role in the process of liver regeneration by terminating hepatocyte proliferation [15]. TGF-β is also involved in liver fibrosis caused by liver injury by promoting the production of extracellular matrix by fibroblasts. TGF-β overexpression is frequently found in HCCs as well as other cancers. Treatment with TGF-β results in the growth arrest of HCC cells expressing TGFBR2 [13], indicating that TGF-β signaling has a tumor-suppressive role in HCC cells as well as normal hepatocytes. Mechanisms to escape TGF-β-induced growth arrest may be necessary for HCC progression.

TGF-β Signaling in HCC

Recently we reported that reduced TGFBR2 expression in HCC correlated with intrahepatic metastasis [13]. Approximately 25% of HCCs showed decreased staining for TGFBR2 compared with adjacent non-cancerous hepatocytes (fig. 1). The TGFBR2 downregulation also correlated with a larger size and higher grade of tumor, and early recurrence time. These findings suggest that TGFBR2 downregulation is a late event in HCC development. TGFBR2-reduced HCC cells exhibited no proliferative response to TGF-β, whereas the growth of TGFBR2-expressing cells was arrested by TGF-β treatment. Thus, the response to TGF-β is TGFBR2-dependent. Although TGFBR2 downregulation seems to be a late event in HCC progression, some cases with a small HCC (≤2 cm) showed reduced TGFBR2 expression (6/60 small HCCs). Two of these cases demonstrated an early recurrence after surgery [unpubl. data], suggesting that reduced TGFBR2 expression may be a risk factor for early recurrence, even in patients with a small HCC.

Mutations and deletions of TGF-β signaling-related genes are found in some cancers. The SMAD4 gene is lost or mutated in about 50% of pancreatic carcinomas [16], and the TGFBR2 gene is mutated in hereditary non-polyposis colorectal carcinoma [17]. Alterations of

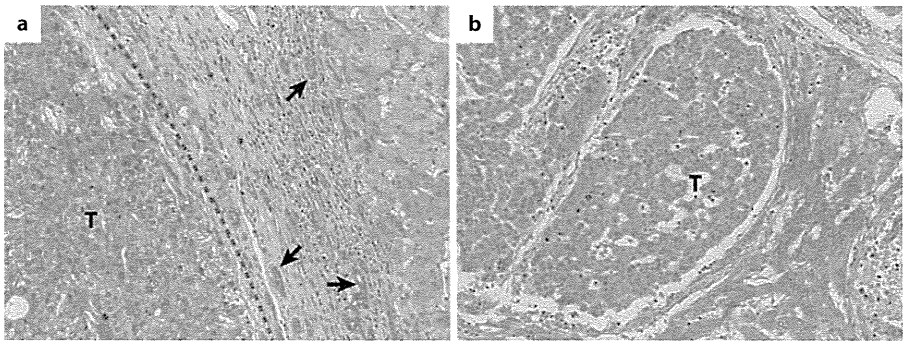

Fig. 1. Immunohistochemical detection of TGFBR2 in HCC tissues. Tumor cells with (**a**) or without (**b**) staining of TGFBR2. Non-neoplastic hepatocytes and cholangiocytes (arrows) showed positive staining for TGFBR2. The dotted line shows the boundary of the tumor (T).

these genes are, however, rare in HCC. Although reduced TGFBR2 expression, which results in suppression of TGF-β-induced growth arrest, has been found in about 25% of HCCs, TGF-β seems to be a tumor suppressor in the majority of HCCs expressing TGFBR2.

TGF-β inhibits cell proliferation, but it also promotes tumor cell invasion by inducing epithelial-mesenchymal transition (EMT) [18]. Coulouarn et al. [19] described the molecular classification of HCC based on the clinical significance of the genes embedded in the TGF-β expression signature. In their study, they examined HCC cell lines using a clustering analysis of microarray data. They found that the early or late response of the cells to TGF-β was a key factor to subclassifying HCC. Genes in the late TGF-β signature include vimentin and Snail, which are characteristic of EMT, suggesting that TGF-β signaling is involved in the EMT of HCC cells. In their study, the HCC cell lines, HLE and HLF, were classified into the late TGF-β subgroup. On the other hand, HLE and HLF cells appear to be negative for TGFBR1 and have a low level of TGFBR2, and growth inhibition with TGF-β is not observed in these cells [20]. These findings suggest that the late response to TGF-β may be independent of the expression of TGF-β receptors. Reduced expression of TGF-β receptor may be a key to shift the TGF-β expression signature from the early to the late response.

TGF-β signaling is also involved in angiogenesis during cancer progression. Ito et al. [21] showed that plasma TGF-β levels correlate positively with tumor vascularity. Mazzocca et al. [22] demonstrated that crosstalk between HCC and endothelial cells was blocked with LY210976, an inhibitor of TGFBR1, by suppressing angiogenesis through vascular endothelial growth factor (VEGF). VEGF is a gene involved in the late response to TGF-β [19]. Thus, TGF-β promotes HCC cells to secrete VEGF, which induces hypervascularization, one of the features of advanced HCC.

Whereas TGF-β phosphorylates the C-terminal region of R-SMADs, MAPK phosphorylates the linker region of R-SMADs [23]. Mori et al. [24] showed that hepatocyte growth factor (HGF) and TGF-β induce R-SMAD phosphorylation at linker regions by JNK, one of the mediators of MAPK pathway. The nuclear accumulation of R-SMAD with a phosphorylated linker region is involved in invasion. Coulouarn et al. [19] demonstrated that HCC cells with the late TGF-β signature expressed genes characteristic of TGF-β-induced metastasis and EMT. These findings led to the hypothesis that the phosphorylation of R-SMAD at the C-terminal or linker region may be reflected in the early or late gene response to TGF-β. In other words, switching the gene response to TGF-β may be implicated in the phosphorylation status of R-SMAD.

Coulouarn et al. [19] identified that the HCC group harboring both the late TGF-β and positive HGF/MET signature is characterized by poor survival. HGF is expressed at significant levels in HCCs, and is primarily expressed by stromal myofibroblasts [25]. Pathologically characteristic differences between early and advanced HCCs are hypervascularization and stromal formation. Since TGF-β induces the transformation of myofibroblasts [26], HCC cells expressing TGF-β can obtain HGF secreted by myofibroblasts surrounding the tumor. Moreover, TGF-β-induced angiogenesis may increase HGF levels in hypervascularized HCC. HGF activates JNK, which in turn phosphorylates R-SMADs at the linker region [24]. Thus, the JNK–SMAD pathway may predominate in advanced HCC.

Conclusion

Alterations of TGF-β levels and TGF-β signaling in multistep hepatocarcinogenesis appear very complex, but they seem to have a significant impact on the molecular

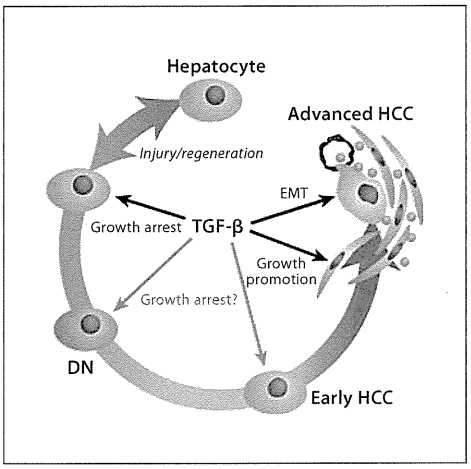

Fig. 2. Role of TGF-β during multistep hepatocarcinogenesis. TGF-β inhibits the proliferation of premalignant hepatocytes and early HCCs, whereas it promotes stromal formation. In HCC cells with the late response to TGF-β, TGF-β contributes to tumor invasion through tumor-stromal interaction.

pathogenesis of HCC. Figure 2 shows a scheme for the role of TGF-β in multistep carcinogenesis. TGF-β signaling has a suppressive role in the proliferation of premalignant hepatocytes and possibly also early HCC cells. In advanced HCCs, TGF-β is involved in the formation of tumor stroma, including myofibroblasts and blood vessels. The stroma provides the microenvironment, including HGF, favorable for tumor cells. In advanced HCC, with such a microenvironment, the early response to TGF-β may shift to the late response, and TGF-β signaling cannot function as a tumor suppressor any longer. Reduced TGFBR2 expression in HCC cells may contribute to suppressing the early TGF-β response, and enhancing the late response.

Disclosure Statement

The are no conflicts of interest to declare.

References

1 World Health Organization (WHO). Cancer. Fact Sheet No. 297. http://www.who.int/mediacentre/factsheets/fs297/en/index.html (2009).
2 Yuen MF, Hou JL, Chutaputti A: Asia-Pacific Working Party on Prevention of Hepatocellular Carcinoma: Hepatocellular carcinoma in the Asia-Pacific region. J Gastroenterol Hepatol 2009;24:346–353.
3 Oda T, Tsuda H, Sakamoto M, Hirohashi S: Different mutations of the *p53* gene in nodule-in-nodule hepatocellular carcinoma as a evidence for multistage progression. Cancer Lett 1994;83:197–200.
4 Qin L, Tang Z, Ma Z, Wu Z, Zhou X, Ye Q, Ji Y, Huang L, Jia H, Sun H, Wang L: p53 immunohistochemical scoring: an independent prognostic marker for patients after hepatocellular carcinoma resection. World J Gastroenterol 2002;8:459–463.
5 Hui AM, Sakamoto M, Kanai Y, Ino Y, Gotoh M, Yokota J, Hirohashi S: Inactivation of p16INK4 in hepatocellular carcinoma. Hepatology 1996;24:575–579.
6 Nakanishi K, Sakamoto M, Yamasaki S, Todo S, Hirohashi S: Akt phosphorylation is a risk factor for early disease recurrence and poor prognosis in hepatocellular carcinoma. Cancer 2005;103:307–312.
7 Chuma M, Sakamoto M, Yamazaki K, Ohta T, Ohki M, Asaka M, Hirohashi S: Expression profiling in multistage hepatocarcinogenesis: identification of HSP70 as a molecular marker of early hepatocellular carcinoma. Hepatology 2003;37:198–207.
8 Shibata R, Mori T, Du W, Chuma M, Gotoh M, Shimazu M, Ueda M, Hirohashi S, Sakamoto M: Overexpression of cyclase-associated protein 2 in multistage hepatocarcinogenesis. Clin Cancer Res 2006;12:5363–5368.
9 Shirai Y, Kawata S, Tamura S, Ito N, Tsushima H, Takaishi K, Kiso S, Matsuzawa Y: Plasma transforming growth factor-β_1 in patients with hepatocellular carcinoma. Comparison with chronic liver diseases. Cancer 1994;73:2275–2279.
10 Bissell DM, Roulot D, George J: Transforming growth factor-β and the liver. Hepatology 2001;34:859–867.
11 Okumoto K, Hattori E, Tamura K, Kiso S, Watanabe H, Saito K, Saito T, Togashi H, Kawata S: Possible contribution of circulating transforming growth factor-β_1 to immunity and prognosis in unresectable hepatocellular carcinoma. Liver Int 2004;24:21–28.
12 Teicher BA: Malignant cells, directors of the malignant process: role of transforming growth factor-β. Cancer Metastasis Rev 2001;20:133–143.
13 Mamiya T, Yamazaki K, Masugi Y, Mori T, Effendi K, Du W, Hibi T, Tanabe M, Ueda M, Takayama T, Sakamoto M: Reduced transforming growth factor-β receptor II expression in hepatocellular carcinoma correlates with intrahepatic metastasis. Lab Invest 2010;90:1339–1345.
14 Heldin CH, Miyazono K, ten Dijke P: TGF-β signalling from cell membrane to nucleus through SMAD proteins. Nature 1997;390:465–471.
15 Dooley S, Weng H, Mertens PR: Hypotheses on the role of transforming growth factor-β in the onset and progression of hepatocellular carcinoma. Dig Dis 2009;27:93–101.
16 Hahn SA, Schutte M, Hoque AT, Moskaluk CA, da Costa LT, Rozenblum E, Weinstein CL, Fischer A, Yeo CJ, Hruban RH, Kern SE: DPC4, a candidate tumor suppressor gene at human chromosome 18q21.1. Science 1996;271:350–353.
17 Markowitz S, Wang J, Myeroff L, Parsons R, Sun L, Lutterbaugh J, Fan RS, Zborowska E, Kinzler KW, Vogelstein B: Inactivation of the type II TGF-β receptor in colon cancer cells with microsatellite instability. Science 1995;268:1336–1338.
18 Thiery JP, Sleeman JP: Complex networks orchestrate epithelial-mesenchymal transitions. Nat Rev Mol Cell Biol 2006;7:131–142.
19 Coulouarn C, Factor VM, Thorgeirsson SS: Transforming growth factor-β gene expression signature in mouse hepatocytes predicts clinical outcome in human cancer. Hepatology 2008;47:2059–2067.
20 Damdinsuren B, Nagano H, Kondo M, Natsag J, Hanada H, Nakamura M, Wada H, Kato H, Marubashi S, Miyamoto A, Takeda Y, Umeshita K, Dono K, Monden M: TGF-β_1-induced cell growth arrest and partial differentiation is related to the suppression of Id1 in human hepatoma cells. Oncol Rep 2006;15:401–408.

21 Ito N, Kawata S, Tamura S, Shirai Y, Kiso S, Tsushima H, Matsuzawa Y: Positive correlation of plasma transforming growth factor-β_1 levels with tumor vascularity in hepatocellular carcinoma. Cancer Lett 1995;89:45–48.
22 Mazzocca A, Fransvea E, Lavezzari G, Antonaci S, Giannelli G: Inhibition of transforming growth factor-β receptor I kinase blocks hepatocellular carcinoma growth through neoangiogenesis regulation. Hepatology 2009;50:1140–1051.
23 Kretzschmar M, Liu F, Hata A, Doody J, Massagué J: The TGF-β family mediator Smad1 is phosphorylated directly and activated functionally by the BMP receptor kinase. Genes Dev 1997;11:984–995.
24 Mori S, Matsuzaki K, Yoshida K, Furukawa F, Tahashi Y, Yamagata H, Sekimoto G, Seki T, Matsui H, Nishizawa M, Fujisawa J, Okazaki K: TGF-β and HGF transmit the signals through JNK-dependent Smad2/3 phosphorylation at the linker regions. Oncogene 2004;23:7416–7429.
25 Guirouilh J, Le Bail B, Boussarie L, Balabaud C, Bioulac-Sage P, Desmoulière A, Schuppan D, Rosenbaum J: Expression of hepatocyte growth factor in human hepatocellular carcinoma. J Hepatol 2001;34:78–83.
26 Dooley S, Delvoux B, Lahme B, Mangasser-Stephan K, Gressner AM: Modulation of transforming growth factor-β response and signaling during transdifferentiation of rat hepatic stellate cells to myofibroblasts. Hepatology 2000;31:1094–1106.

Hepatology Research

Hepatology Research 2011; 41: 240–249 doi: 10.1111/j.1872-034X.2010.00758.x

Original Article

Clinicopathological significance of nuclear factor-κB activation in hepatocellular carcinoma

Hideki Yokoo,[1,2] Jun Yasuda,[1,3]* Kazuaki Nakanishi,[1,2] Makoto Chuma,[1,4] Toshiya Kamiyama,[2] Satoru Todo,[2] Setsuo Hirohashi[1] and Michiie Sakamoto[1,5]

[1]*Pathology Division, National Cancer Center Research Institute,* [3]*Department of Cell Biology, JFCR Cancer Institute,* [5]*Department of Pathology, Keio University, School of Medicine, Tokyo,* [2]*Department of General Surgery, Hokkaido University, Graduate School of Medicine, and* [4]*Department of Gastroenterology, Hokkaido University, Graduate School of Medicine, Sapporo, Japan*

Aim: Nuclear factor-κB (NF-κB) is a critical signaling mediator in inflammation, apoptosis resistance and oncogenesis. It has been reported that NF-κB is activated in several cancers, including hepatocellular carcinoma (HCC). Studies of genetic disruptions in mice also suggest that NF-κB plays critical roles in hepatocarcinogenesis. The aim of the present study is to characterize NF-κB activation and correlate it with the degree of malignancy in HCC.

Methods: To examine the correlation between the positivity of the nuclear p50 subunit and HCC recurrence, we analyzed immunostaining of the NF-κB p50 subunit in two groups of HCC samples with known prognosis and Akt phosphorylation status: 49 patients showing early recurrence within 6 months (group A) and 50 patients who were recurrence-free for at least for 3 years (group B).

Results: In group A, positive nuclear staining of p50 was shown in 18 cases (36.7%), whereas only one case (2.0%) in group B had positive nuclear staining of p50 ($P = 2.48839 \times 10^{-5}$). This suggests a positive relationship between nuclear p50 and early recurrence and advanced HCC in humans. The presence of phosphorylated Akt correlated with nuclear staining of p50 in HCCs in group A ($R^2 = 0.213$, $P < 0.001$).

Conclusion: Our results indicate that nuclear staining of p50 was clearly associated with early recurrent HCC, and the Akt pathway might play a role in NF-κB activation in a subset of early recurrent HCC.

Key words: clinical significance, hepatocellular carcinoma, immunohistochemistry, nuclear factor-κB, phosphorylated Akt

INTRODUCTION

HEPATOCELLULAR CARCINOMA (HCC) is one of the most common malignancies worldwide and is currently the third leading cause of cancer deaths among males in Japan (Vital Statistics of Japan, Ministry of Health, Labor and Welfare). The prognosis of HCC after initial treatment remains poor because of the high rate of recurrence and hematogenous intrahepatic metastasis.[1,2] Gross pathological types, microscopic vascular invasion and intrahepatic metastasis are risk factors for recurrence and poor prognosis.[3,4] Especially, early intrahepatic recurrences (6 months after initial treatment) often occur as hematogenous metastases and are associated with poorer prognosis. Understanding the molecular mechanisms of hematogenous intrahepatic metastasis is an important step toward the identification of efficient biomarkers and more specific therapeutic or diagnostic targets for HCC recurrence.

Cancer metastasis is a multistep process that involves cell detachment from the primary tumor. In the metastasis process, anchorage-independent growth is clearly important, especially in the liver where cancer cells need to survive with almost no cell–substratum interaction. Our previous report suggests that anchorage-independent growth regulated by the phosphatidylinositol 3-kinase (PI3K)/Akt pathway plays a critical role in the metastasis of HCC.[5] Phosphorylated Akt (pAkt) is the active form of Akt, which inhibits apoptosis through various mechanisms.[6,7] One such mechanism is the activation of nuclear

Correspondence: Dr Jun Yasuda, Department of Cell Biology, JFCR Cancer Institute, 3-8-31 Ariake, Koto-ku, Tokyo 135-8550, Japan. Email: jun.yasuda@jfcr.or.jp
*Jun Yasuda is a COE Fellow at Tohoku University.
Received 16 June 2010; revision 8 September 2010; accepted 24 September 2010.

factor-κB (NF-κB) through the association of Akt with IκB kinase.[8]

Nuclear factor-κB was first identified by Sen and Baltimore[9] as a constitutively active transcription factor that binds to the κ-light chain immunoglobulin enhancer sequence in B lymphocytes. It has been reported that NF-κB plays an important role in the regulation of immune responses, apoptosis, cell proliferation, cell motility, inflammation and oncogenesis.[10] Currently, NF-κB consists of a family of five structurally related and evolutionarily conserved proteins: Rel (c-Rel), RelA (p65), RelB, NF-κB1 (p50 and its precursor p105) and NF-κB2 (p52 and its precursor p100).[11] NF-κB/Rel proteins can exist as homo- or heterodimers in the cytoplasm in an inactive form; the heterodimer is associated with a class of inhibitory molecules, IκB family proteins. Activation of the NF-κB signaling cascade results in degradation of IκB and, subsequently, translocation of NF-κB into the nucleus.[12]

Recent extensive studies with a series of genetic disruptions in mice revealed that the NF-κB pathway is critical for the early and late stages of hepatocarcinogenesis.[13] Especially, the NF-κB pathway is an essential anti-apoptotic factor in hepatocarcinogenesis induced after chronic inflammation of the liver,[14,15] whereas it is suppressive for HCC formation after acute chemical induction of liver inflammation.[16,17] Elevation of NF-κB activity has already been studied in human HCC.[18–20] However, the relationship between the degree of malignancy in HCC and NF-κB activation has not been well characterized, and the histopathological significance of nuclear translocation of NF-κB in HCC has not been well analyzed.

In this study, we identified a polyclonal antibody specific for the p50 subunit of NF-κB that was suitable for immunohistochemistry of paraffin-embedded, formalin-fixed, human liver tissue, and investigated the relationship between nuclear staining of NF-κB and clinicopathological findings, including the presence or absence of pAkt, with our previously reported human HCC specimen consisting of two different groups: 49 patients with early recurrence within 6 months and 50 patients with no recurrence in more than 3 years.[21]

METHODS

Cell culture and reagents

THE HUMAN HCC cell line PLC/PRF/5 was obtained from the American Type Culture Collection. KIM-1 and KYN-2[22] were kindly provided by Dr Masamichi Kojiro (Department of Pathology, Kurume University School of Medicine, Kurume, Japan), and Li7 was established in our laboratory.[23] All cell lines were cultured on collagen-coated dishes in RPMI-1640 supplemented with 10% fetal bovine serum, 100 units/mL penicillin, and 100 μg/mL streptomycin. To observe the nuclear import of NF-κB p50 subunits, recombinant interleukin (IL)-1a protein was purchased (R&D Systems, Minneapolis, MN, USA).

Immunoblots

For immunoblotting, cells were lysed with Triton lysis buffer (137 mM NaCl, 20 mM Tris-Cl [pH 7.4], 1% Triton X-100, 25 mM β-glycerophosphate, 2 mM ethylene diamine tetra acetate [pH 8.0], 0.1 mM sodium orthovanadate, and complete protease inhibitor) (Roche, Mannheim, Germany). The lysate was cleared by centrifugation, and the protein concentration was determined by using the DC Protein Assay (Bio-Rad Laboratories, Hercules, CA, USA). Proteins in the lysates were separated by sodium dodecylsulfate polyacrylamide gel electrophoresis (10% polyacrylamide) and electroblotted to Immobilon, a polyvinylidene difluoride membrane (Millipore, Billerica, MA, USA). Immunoblotting was performed according to the instructions provided by the antibody supplier. The non-specific sites on the membrane were blocked by incubation with blocking buffer (3% [w/v] non-fat dry milk, 1% [w/v] bovine serum albumin, 150 mM NaCl and 15 mM Tris-Cl [pH 7.4]) for 30 min at room temperature. The blocked membrane was incubated with primary antibodies in blocking buffer and followed by washing three times with 0.5% Tween-20 in phosphate buffered saline (PBS). Then, the membrane was incubated with secondary antibodies in blocking buffer and washed. Immune complexes were detected by enhanced chemiluminescence (ECL; GE Healthcare, Buckinghamshire, England).

Immunofluorescence

KIM-1 was cultured on glass coverslips coated with collagen type I, fixed with 4% paraformaldehyde in PBS, and permeabilized with 100% cold methanol at −20°C for 10 min. The coverslips were then treated with 4% bovine serum albumin in Tris-buffered saline containing 0.1% Triton X-100 for 1 h at room temperature and incubated with antihuman NF-κB p50 (N) (Immuno-Biological Laboratories, Gunma, Japan) as the primary antibody at 4°C overnight, followed by incubation with fluorescein isothiocyanate (FITC)-labeled secondary antibody (Vector Laboratories, Burlingame, CA, USA).

Table 1 Clinicopathological parameters of hepatocellular carcinoma patients analyzed in this study

Clinical parameters	Group A ($n = 49$) (%)	Group B ($n = 50$) (%)	*P*-value
Sex			0.624
Male	38 (77.6)	41 (82.0)	
Female	11 (22.4)	9 (18.0)	
Virus infection			4.485×10^{-2}
$HBsAg^+$, $HCVAb^-$	6 (12.2)	11 (22.0)	
$HBsAg^-$, $HCVAb^+$	32 (65.3)	20 (40.0)	
$HBsAg^+$, $HCVAb^+$	3 (6.1)	3 (6.0)	
$HBsAg^-$, $HCVAb^-$	8 (16.3)	16 (32.0)	
Tumor size (cm)	6.63 ± 5.10	4.24 ± 2.35	4.316×10^{-3}
Macroscopic classification			0.016
Early	0 (0.0)	6 (12.0)	
Type 1	10 (20.4)	17 (34.0)	
Type 2	25 (51.0)	17 (34.0)	
Type 3	14 (28.6)	10 (20.0)	
Tumor differentiation (%)			2.639×10^{-5}
Well	2 (4.1)	19 (38.0)	
Moderately	30 (61.2)	25 (50.0)	
Poorly	17 (34.7)	6 (12.0)	
Portal vein invasion (%)			2.832×10^{-11}
Presence	40 (75.5)	8 (16.0)	
Absence	9 (18.4)	42 (84.0)	
No. of intrahepatic metastases			2.815×10^{-27}
>3	37 (75.5)	0 (0.0)	
1 or 2	12 (24.5)	2 (4.0)	
0	0 (0.0)	48 (96.0)	

P-value between p50 positive and negative. HBsAg, hepatitis B surface antigen; HCVAb, hepatitis C virus antibody.

Labeled cells were mounted in Vectashield with DAPI (Vector Laboratories) and examined with a Zeiss LSM410 microscope (Carl Zeiss, Thornwood, NY, USA).

Patients and tissue specimens

For immunohistochemical analysis, all specimens were obtained from patients with HCC, who had undergone initial hepatectomy at the National Cancer Center Hospital (Tokyo, Japan). The HCC patients were divided into two groups: 49 patients showing early recurrence within 6 months (group A), and 50 patients who were recurrence-free for at least 3 years between 1990 and 1999 (group B). The state of pAkt and Ki-67 of those two groups of patients have been reported previously.[21] In addition, 42 consecutive HCC patients (30 men and 12 women) between 1999 and 2000 at the National Cancer Center Hospital were also analyzed to examine the overall frequency and clinicopathological features of the NF-κB-activated HCC (Supplementary Table S1). Gross typing[24] and histological diagnosis were done according to the General Rules for the Clinical and Pathological Study of Primary Liver Cancer (Liver Cancer Study Group of Japan).[25] The main clinical parameters and clinicopathological features are presented in Tables 1 and 3. The use of human subjects for this study was approved by the institutional review board of the National Cancer Center.

Immunohistochemistry

Tumor tissue blocks containing both cancerous and adjacent non-cancerous tissue were selected by macroscopic inspection for further analysis. Samples were fixed with 10% formalin and subsequently embedded in paraffin. Serial sections (thickness 5 μm) were prepared from paraffin blocks. Sections were deparaffinized with xylene and ethanol and treated with 0.3% hydrogen peroxide in methanol to reduce endogenous peroxidase activity. After 0.3% hydrogen peroxide treatment, heat-induced antigen retrieval was performed for 10 min at 121°C in 10 mM citrate buffer (pH 6.0) using an autoclave. The sections were coated with normal swine serum (DAKO, Glostrup, Denmark) for 10 min to block non-specific antibody binding. Subsequently, the blocked sections were incubated with antihuman NF-κB

p50 (N) (1:100) as the primary antibody at 4°C overnight. The sections were then incubated with biotinylated, goat antirabbit immunoglobulin as the secondary antibody (1:200; Vector Laboratories) at room temperature for 1 h. The sections were further treated with the Vectastain Elite ABC Kit (Vector Laboratories) at room temperature for 30 min. Finally, the immune complex was visualized using a peroxidase reaction with 3,3′-diaminobenzidine (Mutoh Chemicals, Tokyo, Japan), followed by nuclear counterstaining with methyl green. The tissue samples were washed three times with PBS after each step.

Immunohistochemical evaluation

We used nuclear staining of lymphocytes as a positive control in the same HCC sections. At least 100 cells were counted in each section, and more than 80% of nuclear staining was considered NF-κB p50 positive. Immunostaining of p50 for lymphocytes was used as an internal control. Nuclear staining was evaluated by two independent pathologists (H. Y. and M. S.). The nuclear p50 staining of HCC were scored as: 0 (no nuclear staining); 1 (weak staining: less than that of infiltrating lymphocytes in HCC); and 2 (strong staining: similar to or more than that of infiltrating lymphocytes in HCC).

Statistical analysis

The differences between clinical and biochemical characteristics were examined using the Mann–Whitney *U*-test or Fisher's exact probability test for discrete variables and Student's *t*-test for continuous variables. Other statistical analyses, such as survival analysis and multiple regression analysis, were done with the R statistical environment (www.r-project.org).

RESULTS

Confirmation of the specificity of anti-p50 antibody

WE TESTED A number of commercially available antibodies against subunits of NF-κB for immunodetection and found that the rabbit polyclonal anti-p50 antibody (IBL) was the most suitable for our study. Immunoblot analysis of a series of HCC cell lines at steady state with the anti-p50 antibody is shown in Figure 1(a). Two distinct bands were observed in each lane. The molecular weights of the lower and higher bands were 50 kDa and 105 kDa, respectively, and the sizes correspond to the NF-κB p50 subunit and its precursor, p105. The band intensity of p50 and p105 proteins was similar in all cell lines except for KYN-2, in which slightly weak signals were obtained (Fig. 1a).

Nuclear factor-κB is sequestered in an inactive form in the cytoplasm and is then translocated to the nucleus when activated by cytokines. Immunofluorescence analysis with the anti-p50 antibody of KIM-1 cells at steady state revealed that most of the signal derived from the FITC-labeled immune complex was localized in the cytoplasm (Fig. 1b, left panel). Six hours after addition of recombinant IL-1 (20 ng/mL) to the medium, the FITC signal was localized mainly in the nucleus with various cytoplasmic signals (Fig. 1b). In addition, we could observe prominent immunostaining generated by the anti-p50 antibody in the lymph follicles of surgically resected normal spleen and lymphocytes in non-cancerous liver with HCC (data not shown and Supplementary Fig. S1a). We have tried the antibodies against the p65 subunit for the immunohistochemistry of human HCC specimens but failed to observe positive signals. This is consistent with a previous report.[20]

Immunohistochemistry of NF-κB (p50) in HCC

Table 1 provides a summary of the HCC patients (groups A and B, total 99 cases) analyzed in this study. Five clinical parameters showed statistically significant differences between groups A and B: tumor differentiation, virus infection pattern, tumor size, tumor metastasis and portal vein invasion (Table 1). Then, we examined immunostaining of p50 in samples from groups A ($n = 49$, early recurrence ≤6 months) and B ($n = 50$, recurrence-free for ≥3 years) to determine the clinical significance of nuclear staining of p50. The representative staining of nuclear p50 in HCC is shown in Figure 2. The weak cytoplasmic staining of p50 in HCC may indicate the presence of inactive p50 or the p105 precursor, or both, as the cytoplasmic signal was seen in the immunofluorescence analysis of p50 in cultured cells (Fig. 1). Non-tumor background livers did not show nuclear staining of p50 (Fig. 2 and Supplementary Fig. S1a,b). A significantly less frequent p50 nuclear staining was observed in samples from group B than in those from group A (Table 2). Nuclear staining of p50 was positive in 18 patients from group A (36.7%) and in one patient from group B (2.0%), as shown in Table 2. In addition, we analyzed NF-κB p50 nuclear staining in samples from 42 consecutive patients. We found that the nuclear staining of p50 was positive in 26.2% of the cases (Supplementary Table S1 and Supplementary Fig. S1b).

Then, we examined the relationship between positive nuclear staining of p50 and the clinicopathological

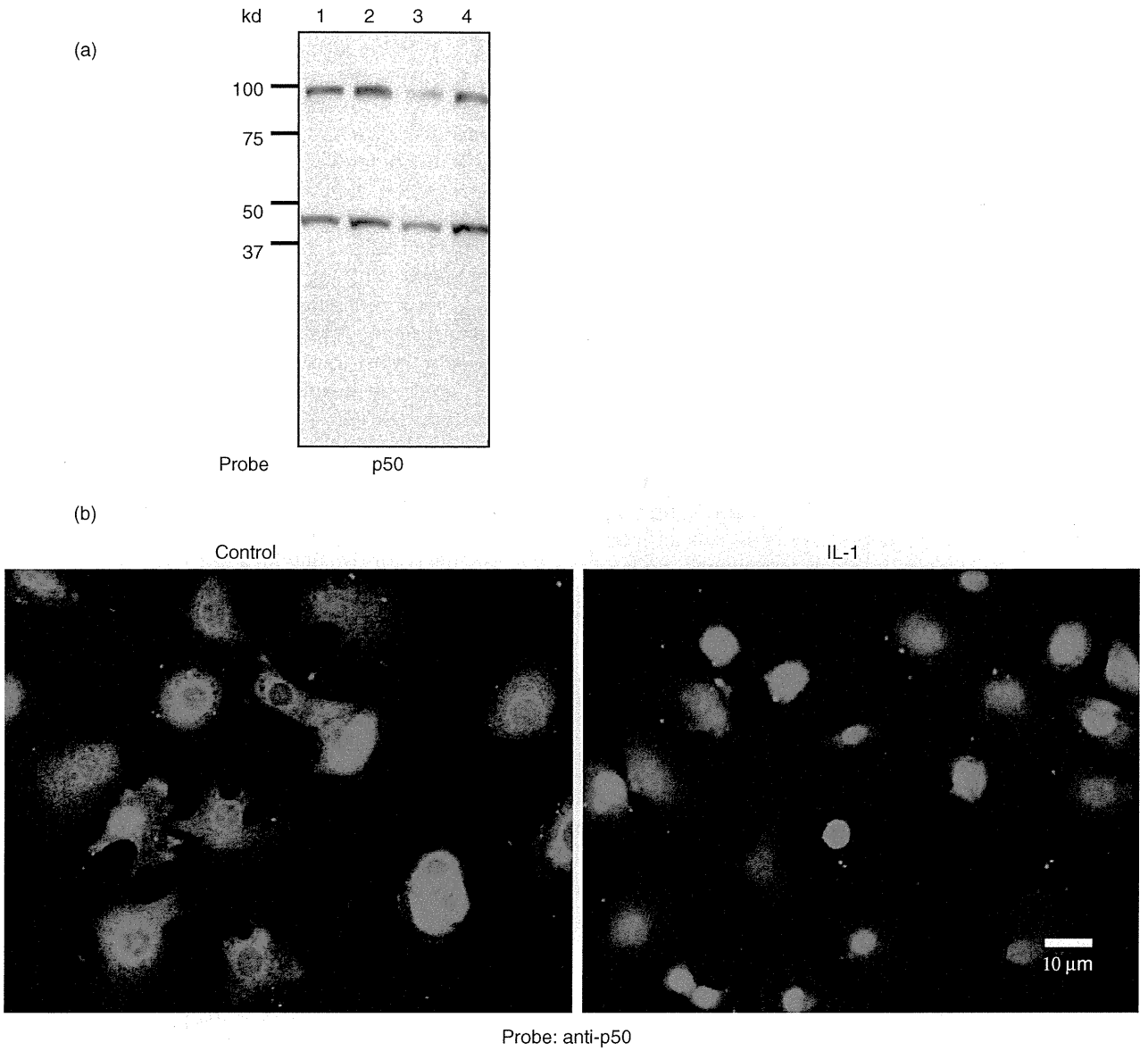

Figure 1 Specificity of anti-p50 antibody. (a) Immunoblotting of cell lysates from human hepatocellular carcinoma cell lines with anti-p50 antibody. Using anti-p50 antibodies, 30 μg of whole cell lysates from PLC/PRF/5 (lane 1), KIM-1 (lane 2), Li7 (lane 3) and KYN-2 (lane 4) were analyzed. (b) Immunofluorescence analysis of KIM-1 cells at the basal state with anti-p50 antibody revealed that most of the fluorescein isothiocyanate (FITC) signal was localized in the cytoplasm. Six hours after the addition of recombinant interleukin (IL)-1 (20 ng/mL) to the medium, the FITC signal was mainly localized to the nucleus of KIM-1 cells. This shift in the FITC staining signal also indicated that the anti-p50 antibody recognized the nuclear factor-κB subunit.

findings of group A. Table 3 summarizes the clinicopathological findings of group A. No obvious correlation was observed between p50 positive HCC and other clinicopathological findings, including recurrence-free survival time after surgery in group A HCC (Table 3). Among the 18 p50 positive group A HCC, staining in seven cases and 11 cases were scored as 1 (weak staining) and 2 (strong staining), respectively (Table 3). We observed homogeneous staining of p50 among HCC cells in a tumor mass and did not find strong heterogeneity in each p50 positive HCC (Figs 1,2).

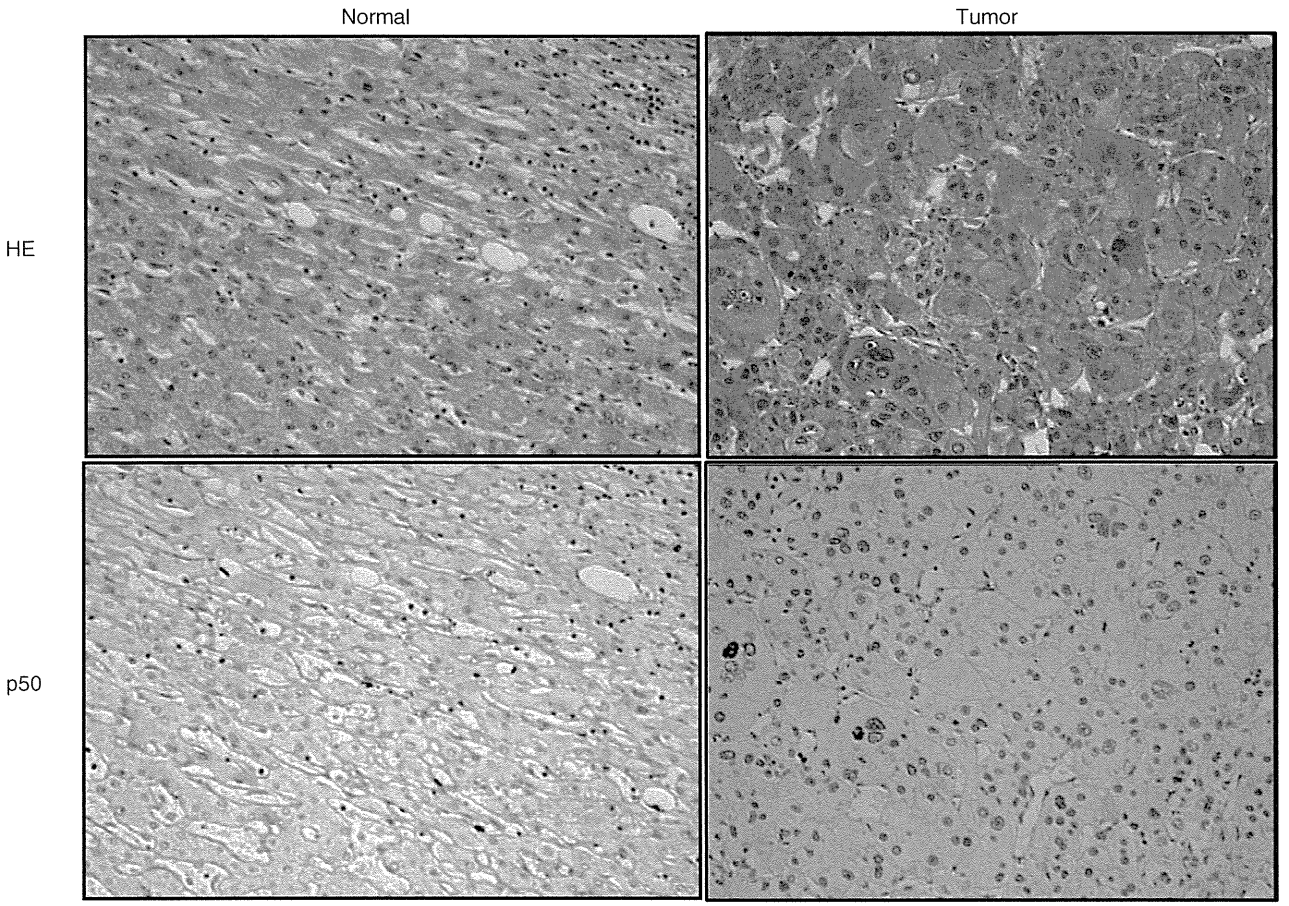

Figure 2 Representative pattern of immunohistological expression of p50 in hepatocellular carcinoma (HCC) and in surrounding non-cancerous tissue (original magnification ×200). Nuclear staining of p50 in a HCC sample from a patient in the early recurrent case group (group A). Compared with the non-cancerous portion of the section (left panels), nuclear staining of the p50 subunit was positive in the tumor portion (right panels). This representative staining of nuclear p50 was judged as class 2. HE, hematoxylin–eosin.

pAkt is associated with nuclear staining of p50 in HCC

The samples in groups A and B have been previously characterized. pAkt protein staining in these samples correlated with early recurrence of HCC after surgery.[21] Therefore, we examined the correlation between immunostaining of p50 and pAkt in the same samples.[21] pAkt was positive in nine (47.4%) of 19 cases that were p50 positive, but only in four (4.76%) of 80 cases that were p50 negative (Table 4). The pAkt positive cases significantly overlapped with the p50 positive cases

Table 2 Comparison of immunohistochemistry of the nuclear factor (NF)-κB p50 subunit among the hepatocellular carcinoma groups

NF-κB p50	Group A ($n = 49$) (%)	Group B ($n = 50$) (%)	*P*-value
Negative	31 (63.3)	49 (98.0)	5.85×10^{-6}
Positive	18 (36.7)	1 (2.0)	
p50 = 1	7 (14.3)	0 (0.0)	
p50 = 2	11 (22.4)	1 (2.0)	

P-value between p50 positive and negative.

Table 3 Correlations between p50 immunoreactive activity and pathological parameters in group A hepatocellular carcinoma patients

p50 nuclear staining	All positive ($n = 18$)	p50 = 1 ($n = 7$)	p50 = 2 ($n = 11$)	Negative ($n = 31$)	*P*-value*
Tumor size (cm)	7.66 ± 5.37	8.74 ± 6.00	6.96 ± 4.80	6.04 ± 4.84	0.333
Gross classification (%)					0.371
Type 1	5 (27.8)	2 (28.6)	3 (27.3)	5 (16.1)	
Type 2	9 (50.0)	3 (42.9)	6 (54.5)	16 (51.6)	
Type 3	4 (22.2)	2 (28.6)	2 (18.2)	10 (32.3)	
Tumor differentiation (%)					0.095
Well	0 (0.0)	0 (0.0)	0 (0.0)	2 (6.5)	
Moderately	10 (55.6)	5 (71.4)	5 (45.5)	20 (64.5)	
Poorly	8 (44.4)	2 (28.6)	6 (54.5)	9 (29.0)	
Tumor encapsulation(%)					1.000
Presence	18 (100.0)	7 (100.0)	11 (100.0)	28 (90.3)	
Absence	0 (0.0)	0 (0.0)	0 (0.0)	1 (3.2)	
Unknown	0 (0.0)	0 (0.0)	0 (0.0)	2 (6.5)	
Tumor capsule infiltration (%)					1.000
Presence	12 (66.7)	6 (85.7)	6 (54.5)	18 (58.1)	
Absence	6 (33.3)	1 (14.3)	5 (45.5)	11 (35.5)	
Unknown	0 (0.0)	0 (0.0)	0 (0.0)	2 (6.5)	
Portal vein invasion (%)					0.127
Presence	17 (94.4)	7 (100.0)	10 (90.9)	23 (74.2)	
Absence	1 (5.6)	0 (0.0)	1 (9.1)	8 (25.8)	
Intrahepatic metastasis (%)					1.00
Presence	14 (77.8)	5 (71.4)	9 (81.8)	23 (74.2)	
Absence	4 (22.2)	2 (28.6)	2 (18.2)	8 (25.8)	
Background liver (%)					0.785
Normal	3 (16.7)	2 (28.6)	1 (9.1)	2 (6.5)	
Chronic hepatitis	5 (27.8)	2 (28.6)	3 (27.3)	16 (51.6)	
Pre-cirrhosis	5 (27.8)	2 (28.6)	3 (27.3)	5 (16.1)	
Cirrhosis	5 (27.8)	1 (14.3)	4 (36.4)	8 (25.8)	
Types of recurrence (%)					1.00
Singular	4 (22.2)	1 (14.3)	3 (27.3)	8 (25.8)	
Multiple	14 (77.8)	6 (85.7)	8 (72.7)	23 (74.2)	
Months of survival after onset	15.1 ± 14.4	10.3 ± 4.72	18.1 ± 17.4	16.5 ± 10.8	0.675

Continuous data are expressed as mean ± standard deviation.
**P*-value between p50 positive and negative.

Table 4 Correlation between immunostaining of nuclear factor (NF)-κB p50 and phosphorylated Akt (pAkt) in groups A and B

		NF-κB p50		
		Positive	Negative	Total
pAkt	Positive	9	4	13
	Negative	10	76	86
	Total	19	80	99

$P = 2.48839 \times 10^{-5}$.

($P = 2.48839 \times 10^{-5}$, Fisher's exact test). Based on linear regression analyses, the presence of pAkt was correlated with nuclear staining of p50 in HCC in group A ($R^2 = 0.213$, $P < 0.001$) but the Ki-67 staining was not ($R^2 = 0.00337$, $P > 0.69$). To further investigate the relationship between pAkt and NF-κB p50 staining, we used multiple regression analyses with Akaike's Information Criteria for p50 staining with several clinicopathological parameters, such as pAkt staining and T classification in group A patients, and several clinical parameters including pAkt staining were selected as explanatory variables although not all variables showed *P*-values less than 0.01 (data not shown).

DISCUSSION

WE HAVE DEMONSTRATED that nuclear staining of the NF-κB p50 subunit was frequently found in early recurrent HCC. The present study suggests that NF-κB is activated in a subset of HCC cases, which may directly contribute to the malignant phenotype of HCC.

Genetic disruptions of the components of the NF-κB pathway contribute to the elucidation of importance in hepatocarcinogenesis induced by the chronic inflammation in mouse models.[14,15] In these model mice, the NF-κB pathway induced the anti-apoptotic genes[14] and cell-growth-stimulating cytokines[15] in HCC cells at the late stage of hepatocarcinogenesis. Thus, it is quite reasonable that nuclear staining of p50 was associated with early recurrent HCC in our collection (Table 2). In the present study, however, one HCC sample showed positive nuclear staining of p50 in group B. The nuclear localizations of NF-κB subunits were also observed with well-differentiated, early-stage HCC in previous reports.[18–20] Our results are compatible with these previous studies. We failed to see the correlation with nuclear staining of p50 and Ki-67 in group A of our collection. It is possible that NF-κB activation mainly functions for protection from apoptotic cell death in hepatocarcinogenesis in the HCC with nuclear p50 staining. We may need to perform further analyses on other factors of NF-κB, such as pro-apoptotic molecules, which might block the progression of disease by counteracting against the constitutive active NF-κB and in the well-differentiated, not recurrent, HCC. In terms of prognosis, nuclear staining of a subunit of NF-κB, p52, showed the correlations with poor prognosis in HCC.[20] However, we did not see clear correlation with nuclear staining of p50 and prognosis in group A of our collection (data not shown). One obvious reason is that the cases in a previous study[20] were 30 sequential patients whereas our group A consisted of early recurrent cases only. Further studies will be needed to clarify if the p50 nuclear staining is an efficient prognostic marker for the HCC.

In terms of pAkt in HCC, a previous study reported 79.7% pAkt immunostaining in 69 cases of HCC[26] compared with 26.5% in our previous cases.[21] This highly frequent pAkt positivity has been reported for many other cancers (see review by Altomare and Testa).[27] The reason for the very large difference in the frequency of pAkt in HCC between the two studies is unknown. However, it might be possible that the sensitivity of the analysis by Perukides *et al.*[26] was higher than that of our previous study.[21]

The present study indicates that most pAkt positive HCC cases found in the previous study showed nuclear staining of NF-κB p50. These results are in accordance with the previous observation that activated Akt could stimulate the NF-κB pathway in anti-apoptotic signaling.[8] Notably, half of the cases that showed nuclear staining of p50 did not show pAkt staining. Considering the higher frequency of pAkt detection in HCC reported by another group,[26] one obvious possibility is that our previous study[21] underestimated the positivity of pAkt, and most of the NF-κB would have been activated by pAkt. Alternatively, this result can mean that other survival pathways might activate NF-κB. Some studies have shown Akt-independent activation of NF-κB.[28,29] There are several candidate NF-κB activators besides Akt, such as casein kinase II, that can directly phosphorylate IκBα.[30,31] It is also possible that the association between pAkt and nuclear staining of p50 in our collection is a mere coincidence. Searching for other activators of NF-κB in HCC than Akt may be important for understanding liver carcinogenesis.

Finally, our results suggest that nuclear staining of NF-κB p50 is a potential biological marker for early recurrence of HCC after surgery. For example, the p50 staining may be beneficial to the surgically resected HCC patients: the nuclear p50 positive HCC patients may be subjected to more frequent checkups after surgery to find early recurrence. Our findings are also suggestive for designing better chemotherapy of early recurrent HCC. The combined treatment of HCC with a proteasome inhibitor bortezomib and a broad-spectrum protein kinase inhibitor, sorafenib, may suppress the Akt activity in HCC.[32] Recently, a suppressor of NEDD8-activating enzyme, MLN4924, was able to inactivate NF-κB in B-cell lymphoma.[33] These new drugs may improve the prognosis of early recurrent HCC after surgery by suppressing the Akt/NF-κB pathway in HCC. We may need to accumulate further cases for the establishment of p50 nuclear staining as a marker of metastatic potential and prognosis of HCC.

ACKNOWLEDGEMENTS

THIS WORK WAS supported by a grant from the Ministry of Health, Labor and Welfare and by the Program for Promotion of Fundamental Studies in Health Sciences of the National Institute of Biomedical Innovation of Japan.

REFERENCES

1 Nagao T, Inoue S, Goto S *et al.* Hepatic resection for hepatocellular carcinoma. Clinical features and long-term prognosis. *Ann Surg* 1987; **205**: 33–40.
2 Nagao T, Inoue S, Yoshimi F *et al.* Postoperative recurrence of hepatocellular carcinoma. *Ann Surg* 1990; **211**: 28–33.
3 Hui AM, Takayama T, Sano K *et al.* Predictive value of gross classification of hepatocellular carcinoma on recurrence and survival after hepatectomy. *J Hepatol* 2000; **33**: 975–9.
4 Shimada M, Hasegawa H, Gion T *et al.* Risk factors of the recurrence of hepatocellular carcinoma originating from residual cancer cells after hepatectomy. *Hepatogastroenterology* 1999; **46**: 2469–75.
5 Nakanishi K, Sakamoto M, Yasuda J *et al.* Critical involvement of the phosphatidylinositol 3-kinase/Akt pathway in anchorage-independent growth and hematogeneous intrahepatic metastasis of liver cancer. *Cancer Res* 2002; **62**: 2971–5.
6 Kandel ES, Hay N. The regulation and activities of the multifunctional serine/threonine kinase Akt/PKB. *Exp Cell Res* 1999; **253**: 210–29.
7 Datta SR, Brunet A, Greenberg ME. Cellular survival: a play in three Akts. *Genes Dev* 1999; **13**: 2905–27.
8 Romashkova JA, Makarov SS. NF-kappaB is a target of AKT in anti-apoptotic PDGF signalling. *Nature* 1999; **401**: 86–90.
9 Sen R, Baltimore D. Inducibility of kappa immunoglobulin enhancer-binding protein Nf-kappa B by a posttranslational mechanism. *Cell* 1986; **47**: 921–8.
10 Chen F, Castranova V, Shi X. New insights into the role of nuclear factor-kappaB in cell growth regulation. *Am J Pathol* 2001; **159**: 387–97.
11 Zhang G, Ghosh S. Toll-like receptor-mediated NF-kappaB activation: a phylogenetically conserved paradigm in innate immunity. *J Clin Invest* 2001; **107**: 13–9.
12 Baeuerle PA, Baltimore D. I kappa B: a specific inhibitor of the NF-kappa B transcription factor. *Science* 1988; **242**: 540–6.
13 Sun B, Karin M. NF-kappaB signaling, liver disease and hepatoprotective agents. *Oncogene* 2008; **27**: 6228–44.
14 Pikarsky E, Porat RM, Stein I *et al.* NF-[kappa]B functions as a tumour promoter in inflammation-associated cancer. *Nature* 2004; **431**: 461–6.
15 Haybaeck J, Zeller N, Wolf MJ *et al.* A lymphotoxin-driven pathway to hepatocellular carcinoma. *Cancer Cell* 2009; **16**: 295–308.
16 Maeda S, Kamata H, Luo J-L, Leffert H, Karin M. IKK[beta] couples hepatocyte death to cytokine-driven compensatory proliferation that promotes chemical hepatocarcinogenesis. *Cell* 2005; **121**: 977–90.
17 He G, Yu GY, Temkin V *et al.* Hepatocyte IKKbeta/NF-kappaB inhibits tumor promotion and progression by preventing oxidative stress-driven STAT3 activation. *Cancer Cell* 2010; **17**: 286–97.
18 Tai DI, Tsai SL, Chang YH *et al.* Constitutive activation of nuclear factor kappaB in hepatocellular carcinoma. *Cancer* 2000; **89**: 2274–81.
19 Qiao L, Zhang H, Yu J *et al.* Constitutive activation of NF-kappaB in human hepatocellular carcinoma: evidence of a cytoprotective role. *Hum Gene Ther* 2006; **17**: 280–90.
20 O'Neil BH, Buzkova P, Farrah H *et al.* Expression of nuclear factor-kappaB family proteins in hepatocellular carcinomas. *Oncology* 2007; **72**: 97–104.
21 Nakanishi K, Sakamoto M, Yamasaki S, Todo S, Hirohashi S. Akt phosphorylation is a risk factor for early disease recurrence and poor prognosis in hepatocellular carcinoma. *Cancer* 2005; **103**: 307–12.
22 Genda T, Sakamoto M, Ichida T *et al.* Cell motility mediated by rho and Rho-associated protein kinase plays a critical role in intrahepatic metastasis of human hepatocellular carcinoma. *Hepatology* 1999; **30**: 1027–36.
23 Hirohashi S, Shimosato Y, Kameya T *et al.* Production of alpha-fetoprotein and normal serum proteins by xenotransplanted human hepatomas in relation to their growth and morphology. *Cancer Res* 1979; **39**: 1819–28.
24 Kanai T, Hirohashi S, Upton MP *et al.* Pathology of small hepatocellular carcinoma. A proposal for a new gross classification. *Cancer* 1987; **60**: 810–9.
25 LCSGJ LCSGoJ. *General Rules for the Clinical and Pathological Study of Primary Liver Cancer*, 2nd edn. Tokyo: Kanehara, 2003.
26 Peroukides S, Bravou V, Varakis J, Alexopoulos A, Kalofonos H, Papadaki H. ILK overexpression in human hepatocellular carcinoma and liver cirrhosis correlates with activation of Akt. *Oncol Rep* 2008; **20**: 1337–44.
27 Altomare DA, Testa JR. Perturbations of the AKT signaling pathway in human cancer. *Oncogene* 2005; **24**: 7455–64.
28 Machuca C, Mendoza-Milla C, Cordova E *et al.* Dexamethasone protection from TNF-alpha-induced cell death in MCF-7 cells requires NF-kappaB and is independent from AKT. *BMC Cell Biol* 2006; **7**: 9.
29 Mendoza-Milla C, Machuca Rodriguez C, Cordova Alarcon E *et al.* NF-kappaB activation but not PI3K/Akt is required for dexamethasone dependent protection against TNF-alpha cytotoxicity in L929 cells. *FEBS Lett* 2005; **579**: 3947–52.
30 Romieu-Mourez R, Landesman-Bollag E, Seldin DC, Sonenshein GE. Protein kinase CK2 promotes aberrant activation of nuclear factor-kappaB, transformed phenotype, and survival of breast cancer cells. *Cancer Res* 2002; **62**: 6770–8.
31 Kato T Jr, Delhase M, Hoffmann A, Karin M. CK2 Is a C-Terminal IkappaB Kinase Responsible for NF-kappaB Activation during the UV Response. *Mol Cell* 2003; **12**: 829–39.
32 Chen KF, Yu HC, Liu TH, Lee SS, Chen PJ, Cheng AL. Synergistic interactions between sorafenib and bortezomib in hepatocellular carcinoma involve PP2A-dependent Akt inactivation. *J Hepatol* 2010; **52**: 88–95.

33 Milhollen MA, Traore T, Adams-Duffy J *et al.* MLN4924, a NEDD8-activating enzyme inhibitor, is active in diffuse large B-cell lymphoma models: rationale for treatment of NF-{kappa}B-dependent lymphoma. *Blood* 2010; **116**: 1515–23.

SUPPORTING INFORMATION

ADDITIONAL SUPPORTING INFORMATION may be found in the online version of this article:

Figure S1 (a) Nuclear staining of p50 in lymphocytes infiltrating in the non-cancerous liver of a hepatocellular carcinoma (HCC) patient. Compared with the hepatocytes, nuclear staining of the p50 subunit was clearly evident in the lymphocytes. (b) Nuclear staining of p50 in an HCC sample from a patient in the consecutive case group (see Methods). Compared with the non-cancerous portion of the section (bottom side, indicated as N in the upper panel), the nuclear staining of the p50 subunits was positive in the tumor portion (top side, indicated as T in the upper panel).

Table S1 Correlations between p50 immunoreactivity and pathological parameters in 42 consecutive hepatocellular carcinoma patients

Please note: Wiley-Blackwell are not responsible for the content or functionality of any supporting materials supplied by the authors. Any queries (other than missing material) should be directed to the corresponding author for the article.

Evaluation of the Mean and Entropy of Apparent Diffusion Coefficient Values in Chronic Hepatitis C: Correlation with Pathologic Fibrosis Stage and Inflammatory Activity Grade[1]

Kiminori Fujimoto, MD, PhD
Tatsuyuki Tonan, MD
Sanae Azuma, MD
Masayoshi Kage, MD, PhD
Osamu Nakashima, MD, PhD
Takeshi Johkoh, MD, PhD
Naofumi Hayabuchi, MD, PhD
Koji Okuda, MD, PhD
Takumi Kawaguchi, MD, PhD
Michio Sata, MD, PhD
Aliya Qayyum, MBBS

Purpose: To determine whether mean and entropy apparent diffusion coefficient (ADC) values obtained at diffusion-weighted (DW) magnetic resonance (MR) imaging can help detect and stage histopathologic liver fibrosis and grade inflammation activity in patients with chronic hepatitis C.

Materials and Methods: This retrospective study was approved by the institutional review board, and the requirement for informed consent was waived. The study included 55 patients with focal hepatic lesions and either chronic hepatitis C (n = 43) or normal hepatic function (control subjects) (n = 12). Mean and entropy of volume histograms were generated in four cubic regions of interest placed in the right hepatic lobe of ADC map images, which were obtained at echo-planar DW MR imaging (gradient factor b values of 0 and 1000 sec/mm^2). These two parameters (mean and entropy ADC) were compared by using METAVIR histopathologic liver fibrosis and inflammatory activity scores. Statistical analysis was performed with the Kruskal-Wallis test and receiver operating characteristic curves.

Results: The mean ADC decreased with an increase in the fibrosis stage or inflammatory activity grade, and the entropy ADC increased with an increase in the fibrosis stage or inflammatory activity grade ($P < .001$ for all comparisons, Kruskal-Wallis test). The area under the receiver operating characteristic curve (A_z) for the mean ADC was statistically significant in the differentiation of fibrosis stage or inflammatory activity grade (A_z, 0.807–0.926; $P < .001$ for all comparisons). Entropy of ADC was helpful for classifying normal from abnormal fibrosis stage or inflammatory activity grade (A_z for both parameters, 0.937; $P < .001$).

Conclusion: Assessment of a combination of mean ADC and entropy ADC in patients with chronic hepatitis C is more accurate for predicting pathologic hepatic fibrosis stage and inflammatory activity grade and helpful for detecting early fibrotic or inflammatory activity when compared with assessment of mean ADC alone.

[1] From the Departments of Radiology (K.F., T.T., S.A., N.H.), Diagnostic Pathology (M.K.), Pathology (O.N.), Surgery (K.O.), and Digestive Disease Information and Research (T.K., M.S.), Kurume University School of Medicine, 67 Asahi-machi, Kurume, 830-0011 Japan; Center for Diagnostic Imaging, Kurume University Hospital, Kurume, Japan (K.F.); Department of Radiology, Kinki Central Hospital of Mutual Aid Association of Public School Teachers, Itami, Japan (T.J.); and Department of Radiology, University of California–San Francisco, San Francisco, Calif (A.Q.).
Received April 27, 2010; revision requested June 18; revision received August 16; accepted September 8; final version accepted October 1. **Address correspondence to** K.F. (e-mail: *kimichan@med.kurume-u.ac.jp*).

It is estimated that approximately 400 million people worldwide are infected with the hepatitis C virus (1), with chronic infection in 75%–85% of patients. Once a diagnosis of chronic hepatitis C virus infection is established, cirrhosis develops within 10–20 years in approximately 20% of patients (2). Approximately 50% of patients with chronic hepatitis C fail to achieve a sustained virologic response to standard therapy with PEGylated interferon and ribavirin (3). Disease progression, which may lead to hepatic decompensation, hepatocellular carcinoma, and death, is particularly common in these patients (4,5).

The severity of liver inflammation and fibrosis in patients with chronic hepatitis C is important to consider when making therapeutic decisions and is a useful prognostic indicator. Liver biopsy is the current reference standard used in the assessment of hepatic necroinflammation and fibrosis (6). Several histologic scoring systems are used to evaluate chronic viral hepatitis (7–10). Of these, the METAVIR scoring system was specially designed for determining hepatic fibrosis stage in patients with chronic hepatitis C (10,11). The current focus in clinical practice, however, has shifted from diagnosis alone to risk stratification and disease monitoring (12,13). Liver biopsy is invasive, with a recognized morbidity and mortality, and as such repeated biopsy for the purpose of monitoring disease progression is not the best option. Furthermore, liver biopsies have several inherent limitations, such as sampling error and interobserver variability (6).

Several noninvasive techniques, including biochemical and hematologic tests, a scoring system using a combination of clinical and laboratory tests, ultrasonography (US)–based transient elastography (6,14), and magnetic resonance (MR) imaging (15–24), have been evaluated. Among these, diffusion-weighted (DW) MR imaging has shown promise in the detection and quantification of hepatic fibrosis (18–24) but has not yet been validated as a marker for pathologic hepatic necroinflammation. To our knowledge, semiquantitative analysis of DW MR imaging in the assessment of liver fibrosis has mainly been evaluated by determining the mean apparent diffusion coefficient (ADC) values of regions of interest in liver parenchyma, but volume histogram analyses have not been evaluated. Entropy describes the variation in a volume histogram of ADC and has been shown to have clinical utility for evaluating morphologic changes of organ tissues outside the abdomen (25,26). We postulated that the mean hepatic ADC values and the entropy of hepatic ADC (entropy ADC) values would be helpful for evaluating the alteration in hepatic parenchyma in chronic hepatitis C.

The purpose of this study was to determine whether the mean and entropy ADC values obtained with DW MR imaging can help detect and stage histopathologic liver fibrosis and grade inflammatory activity in patients with chronic hepatitis C.

Advance in Knowledge

- In patients with chronic hepatitis C, entropy of apparent diffusion coefficient (ADC) values might be a sensitive marker for the detection of early hepatic inflammatory activity (median entropy ADC value was 1.23 for an inflammatory activity score of A0 [no activity] and ranged from 1.48 to 1.57 for inflammatory activity scores of A1–A3 [mild to severe activity]) and fibrosis stage (median entropy ADC value was 1.24 for grade F0 fibrosis [no fibrosis] and ranged from 1.36 to 1.64 for grades F1–F4 fibrosis [minimal fibrosis to cirrhosis]).

Implication for Patient Care

- Evaluation of the mean and entropy of liver ADC values obtained with diffusion-weighted MR imaging is a noninvasive method for assessing liver fibrosis stage and inflammatory activity grade and might be used to differentiate early from advanced chronic liver disease; its noninvasiveness allows for repeat performance.

Materials and Methods

Patients

The institutional review board approved this retrospective study and waived the requirement to obtain patient approval or informed consent for the retrospective review of their records and images, which complied with the principles of the Declaration of Helsinki (2008 version) of the World Medical Association (27).

We retrospectively reviewed the medical records and MR images from all patients who underwent assessment of suspected focal hepatic lesions at our institution between June 2006 and May 2007 and who fulfilled the following inclusion criteria: *(a)* patients underwent DW MR imaging, *(b)* pathologic specimens obtained at liver biopsy were adequate for determining the METAVIR score, and *(c)* patients had either chronic active hepatitis C or absence of hepatic dysfunction or viral hepatitis. The patients with an absence of hepatic dysfunction or viral hepatitis were used as control subjects. Chronic active hepatitis C was defined as an established diagnosis of chronic hepatitis C virus infection with detectable anti–hepatitis C virus antibodies and detectable serum

Published online before print
10.1148/radiol.10100853

Radiology 2011; 258:739–748

Abbreviations:
ADC = apparent diffusion coefficient
A_z = area under the receiver operating characteristic curve
CI = confidence interval
DW = diffusion weighted
IQR = 25th to 75th percentile of the interquartile range

Author contributions:
Guarantors of integrity of entire study, K.F., T.T., M.K.; study concepts/study design or data acquisition or data analysis/interpretation, all authors; manuscript drafting or manuscript revision for important intellectual content, all authors; manuscript final version approval, all authors; literature research, K.F., T.T., M.K., T.J., T.K.; clinical studies, K.F., T.T., S.A., M.K., O.N., T.J., N.H., K.O., T.K., M.S.; statistical analysis, K.F.; and manuscript editing, K.F., A.Q.

Potential conflicts of interest are listed at the end of this article.

hepatitis C virus RNA in conjunction with serum aminotransferase levels that remained abnormally high for more than 6 months. Patients were excluded if they had *(a)* a life-threatening extrahepatic condition and *(b)* other causes of chronic liver disease (eg, hepatitis B virus, excessive alcohol consumption [>30 g per day], hemochromatosis, autoimmune hepatitis, Wilson disease, α_1-antitrypsin deficiency, primary sclerosing cholangitis, or primary biliary cirrhosis).

We identified 84 patients who underwent DW MR imaging and METAVIR scoring at our institution. Twenty-nine of those 84 patients were excluded because their chronic liver disease was due to a cause other than the hepatitis C virus (hepatitis B virus in 17 patients and excessive alcohol consumption in 12). Therefore, our final patient population consisted of 55 subjects, including 43 patients with chronic hepatitis C and 12 control subjects without hepatic dysfunction or viral hepatitis. Patients ranged in age from 34 to 83 years (median age, 65 years) and included 35 men and 20 women. The median patient age was 63 years (25th to 75th percentile of the interquartile range [IQR], 59–73 years) for men and 69 years (IQR, 55–72 years) for women. There was no statistically significant difference in age distribution according to sex ($P = .255$, Mann-Whitney U test).

In 48 of the 55 patients (36 patients with chronic hepatitis C and the 12 control subjects), pathologic assessment of the liver was performed by means of surgical biopsy at resection of the focal hepatic lesions (eg, hepatocellular carcinoma or hepatic metastases). In seven of the 55 patients, pathologic assessment of the liver was performed by means of US-guided biopsy with a 17-gauge core biopsy needle. The median interval between DW MR imaging and surgical or core liver biopsy was 7 days (range, 1–14 days).

MR Imaging Techniques and Interpretation

MR imaging was performed at a field strength of 1.5 T (Magnetom Symphony Advanced; Siemens, Erlangen, Germany) with use of a body phased-array coil.

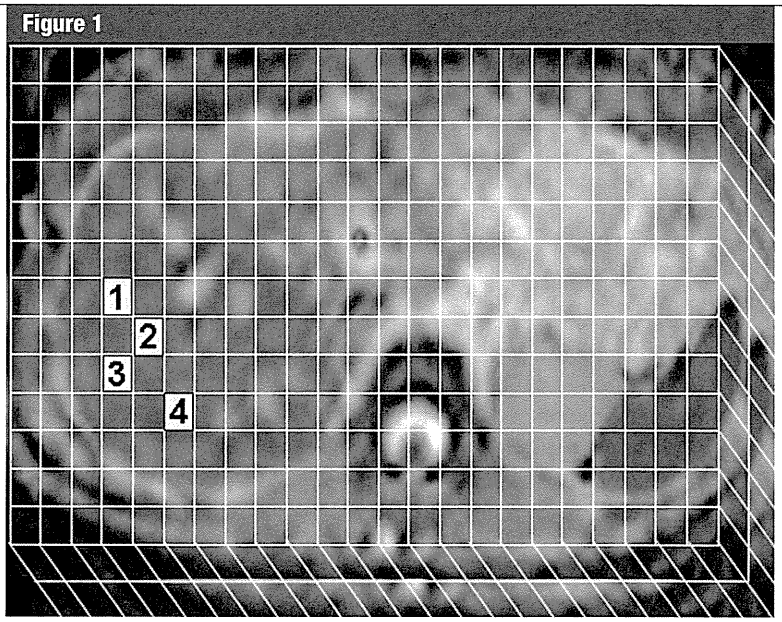

Figure 1: Image illustrates the method used to measure regions of interest on an ADC map. With use of computer software (developed in-house by authors), two independent observers freely and easily selected a region of interest by clicking a mesh unit on the right hepatic lobe of an ADC map image while avoiding the large vessels, focal hepatic lesions, or artifacts. Four cubic regions of interest (3.6 cm^3, approximately 36 voxels) were chosen for liver parenchyma. Numbers on image are regions of interest.

After routine T1- and T2-weighted imaging was performed for the assessment of focal hepatic lesions, a series of respiratory-triggered DW MR images was obtained in all patients.

DW MR imaging was performed in the transverse plane by combining single-shot spin-echo echo-planar imaging with a chemical shift–selective pulse. The imaging parameters for DW MR imaging were as follows: repetition time, 2000 msec; echo time, 81 msec; directions of the motion-probing gradient, three orthogonal axes; gradient factor b values of 0 and 1000 sec/mm^2; 2170-Hz per pixel bandwidth; 350-mm field of view; 128 × 88 rectangular matrixes; 9-mm-thick sections; 1-mm intersection gap; four signals acquired; and acquisition time of approximately 1 minute 30 seconds.

Liver ADC was calculated by using the following equation: $ADC = (-1/b) \times \ln (S_b/S_0)$, where b is the diffusion-sensitizing factor (b value), and S_b and S_0 the signal intensity with and without diffusion weighting, respectively. ADC maps were constructed according to this equation on the basis of a voxelwise calculation.

All regions of interest were determined by two independent observers (T.T. and S.A., with 12 and 8 years of experience, respectively) by using plug-in software developed in-house by two of the authors (K.F. and T.J.) (Fig 1). The two observers were abdominal radiologists who knew that all patients in the study had focal hepatic lesions but were blinded to the other clinical information. Four separate cubic regions of interest (3.6 cm^3, approximately 36 voxels) were manually placed in the anterior and posterior segments of the right hepatic lobe at the level of the porta hepatis (whenever possible) on the calculation ADC maps; care was taken to avoid focal lesions, major vascular structures, and artifacts such as chemical shifts, magnetic susceptibility, and cardiac motion. The regions of interest were drawn in the right hepatic lobe to approximate the regions expected to be sampled for histologic examination.